

MESOSCALE CHARACTERIZATION OF NATURAL AND SYNTHETIC GAS HYDRATES

**Claudia J. Rawn (PI), Hsin Wang, Jane Howe, Michael Lance (Metals and Ceramics Division),
Bryan C. Chakoumakos (Condense Matter Sciences Division), and
Adam J. Rondinone (Chemical Sciences Division)
Oak Ridge National Laboratory
Camille Y. Jones
NIST Center for Neutron Research, Gaithersburg, MD 20899**

INTRODUCTION

Clathrate hydrates are inclusion compounds where a variety of guest molecules can be occluded in a host lattice formed from an ice-like hydrogen bonded network arranged in such a way that polyhedral cavities are created. Two common atomic arrangements that result are cubic and designated as structure I and structure II with unit cell edges of approximately 12 and 17 Å, respectively.

Deposits of natural gas hydrates have been estimated to be several times that of known fossil fuel reserves. In addition to the idea that gas hydrates can be exploited as an energy resource issues surrounding uncontrolled release of the occluded gases into the atmosphere and risks to equipment and personnel resulting from either hydrate plugs in pipelines or reduction in the mechanical strength of the seafloor are of importance.

Prior to this project supported by Fossil Energy our group constructed a pressure cell [1] to synthesize gas hydrates from D₂O and gas and characterize the resulting structures with in-situ neutron powder diffraction with Laboratory Director Research and Development funds. As part of this prior effort we have studied the structure of laboratory synthesized clathrate hydrates of CO₂, CH₄, CH₄-C₂H₆, C₃H₈, TMO, and THF as a function of temperature [2–5]. These atomic structure studies of one or two phase materials (hydrate and ice VII) have aided in understanding the thermal expansion, motion of the occluded molecules, and guest-host interactions of clathrate hydrates. However, these experiments do not provide a complete understanding of the complex multiphase assemblages found in nature where hydrates with several types of gas molecules as the occluded guests are found in a mixture with ice and sediments present as additional phases.

The main emphasis of this project has been to characterize samples found in nature. Natural samples from two different Green Canyon (Gulf of Mexico) locations have been provided by Dr. Roger Sassen (Texas A&M University) and are designated by GC232 and GC234 in this report. Details of sample retrieval and previous characterization by Dr. Sassen and his colleagues can be found at http://www-gerg.tamu.edu/menu_RGD/index.asp.

In the current study, the gas hydrate specimens, GC232 and GC234, were harvested from the mound located at the Green Canyon (GC) in Gulf of Mexico continental slope, southwest of the Mississippi Delta. Visual inspection shows that GC232 contains significant amount of sediment (mud), which appears as white solid (hydrate) with dark gray streaks (sediment) while GC234 (see Fig. 1) is relative pure with little noticeable sediment.



Fig. 1. Natural hydrate sample from Green Canyon in the Gulf of Mexico.

The following report describes characterization of GC232 and CG234 by in-situ x-ray powder diffraction, Small Angle Neutron Scattering (SANS), Inelastic Neutron Scattering (INS), thermal conductivity measurements, IR camera imaging, and Raman studies. Some data will be presented along with preliminary interpretation of the data. Also described are the preparations for a special issue of the American Mineralogist devoted to the clathrate hydrates.

LOW TEMPERATURE X-RAY DIFFRACTION STUDY OF NATURAL HYDRATE SAMPLES

Claudia J. Rawn

INTRODUCTION

We have used low-temperature x-ray powder diffraction to determine the phases present, decomposition temperatures, and the lattice parameters changes as a function of temperature to determine the instantaneous coefficient of thermal expansion in the natural samples designated GC232 and GC234 collected from the Green Canyon in the Gulf of Mexico. Most of the x-ray diffraction data has been analyzed using the Rietveld method which allows structural parameters that are used to calculate powder diffraction patterns to be refined by allowing the parameters to change for the calculated pattern to better fit the observed data. Resulting refined structural parameters include the atomic positions, lattice parameters, site occupancies, and atomic displacement parameters. Additional variables for calculating the diffraction pattern include both sample and instrumental parameters e.g. the peak shape.

EXPERIMENTAL

A laboratory x-ray diffractometer with a theta-theta goniometer has been modified with a closed-cycle He refrigeration unit, vacuum pumping station, and temperature controller. Samples G232 and 234 were loaded onto the low temperature stage in a flowing He glove bag to prevent frosting. The minimum temperature that can be obtained is approximately 12 K and the maximum temperature during loading can be kept under the decomposition temperatures.

The diffraction patterns were collected using $\text{CuK}\alpha$ radiation (45 kV and 40 mA) as step scans with a step size of $0.02^\circ 2\theta$ and a rate of $1^\circ 2\theta/\text{min}$. The sample holder was fabricated from Cu with a deep well for the containment of the samples.

RESULTS AND DISCUSSION

The resulting x-ray powder diffraction patterns showed that both samples were structure II and that ice was present as a secondary phase. In some cases the intensity of the diffraction maxima was not well matched, however the peak positions clearly indicated structure II. Attempts were made to add structure I and the hexagonal form of clathrate

hydrates to the calculated diffraction patterns to account for some of the intensity mismatches, however, calculated patterns with these additional phases did not fit well to the observed data. Most likely the discrepancy in intensities results from the inability to model various gas species in the cages. X-ray powder diffraction data were collected separately on sediments that were included in the samples and is shown in Fig. 2. Phases identified in the sediments included low quartz (SiO_2), aragonite (CaCO_3), and halite (NaCl).

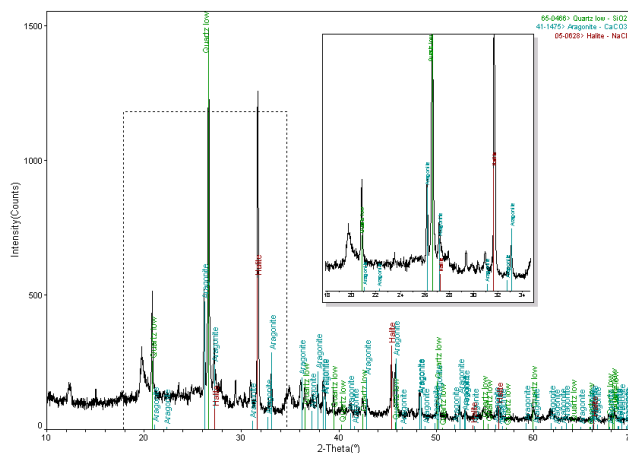


Fig. 2. Ambient temperature x-ray powder diffraction pattern of the sediments included in the natural hydrate samples.

The results shown below are preliminary and several more comparisons need to be made and discussed before any clear conclusions can be made. One result that seems clear is that the natural samples decompose at approximately 190 K. Figure 3 shows the refined a lattice parameter as a function of temperature for two separate runs of sample GC232. Figure 4 shows the wt% ice as a function of temperature for two separate runs of sample GC232 that remains constant at approximately 30 wt% until about 175 K.

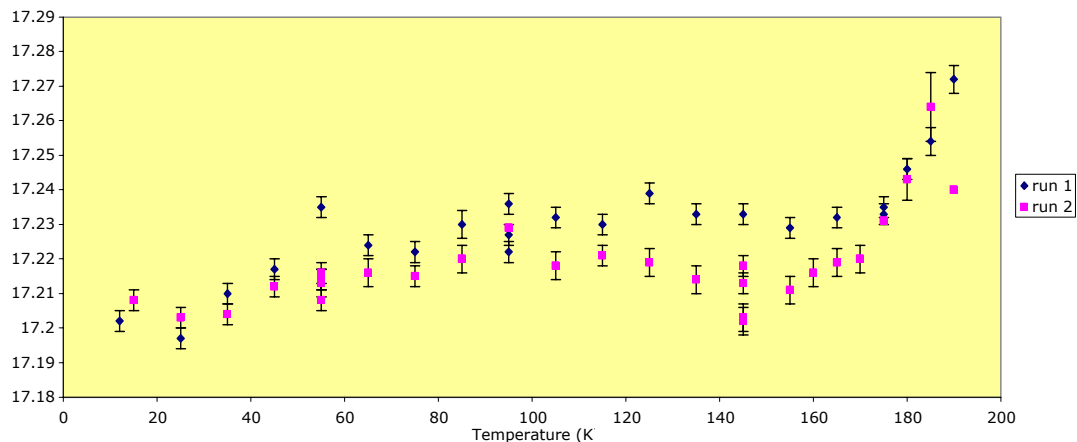


Fig. 3. Refined a lattice parameter as a function of temperature for two separate runs on sample GC232.

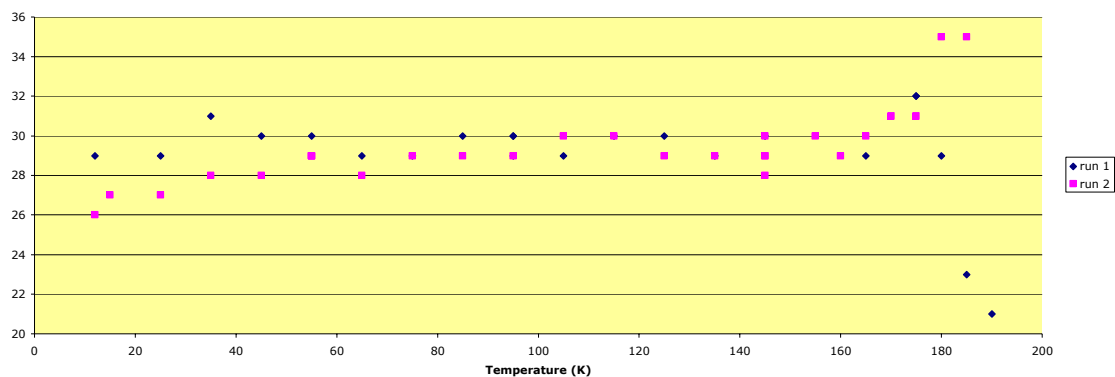


Fig. 4. Weight fraction of ice present as function of temperature for two separate runs on sample GC232.

From the lattice parameter as a function of temperature a/a_0 can be calculated and plotted against temperature and the data fit to a polynomial. By taking the derivate of the polynomial with respect to temperature the instantaneous coefficient thermal expansion can be calculated as shown in Fig. 5 for the two separate runs on sample GC232.

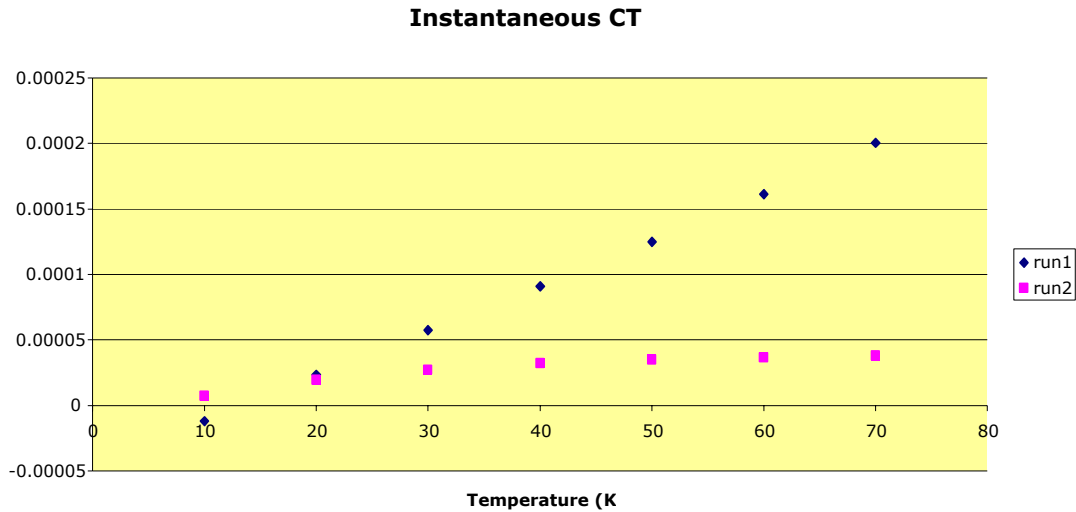


Fig. 5. Instantaneous coefficient of thermal expansion as a function of temperature up to 80 K.

THERMAL CONDUCTIVITY OF NATURAL CLATHRATE HYDRATES IN LIQUID NITROGEN

Hsin Wang

This study is directed at understanding the low temperature thermal transport properties of natural clathrate hydrates.

Two large natural samples were selected for thermal conductivity measurements. The main challenge was to prepare a natural sample with one flat surface, which became a difficult task since the natural samples are shaped like rocks with irregular surfaces, and they have to be kept at very low temperatures. We chose a larger natural sample and wrapped it with aluminum foil, exposing one relatively flat surface for polishing. The sample was quickly taken out of a liquid nitrogen bath and polished on 180 grit sand paper for about 5 seconds and then returned into the liquid nitrogen bath to prevent melting. After repeated polishing cycles, a flat surface was obtained as shown in Fig. 6. In addition to the natural



Fig. 6. Preparation of a flat sample for thermal conductivity measurements.

samples, we also tested ice and TMO structure I samples at liquid nitrogen temperature and compared results with literature values.

THERMAL CONDUCTIVITY MEASUREMENTS

For thermal conductivity measurements, a small piece of Styrofoam and a C-clamp were used to hold the sample and the Hot Disk sensor together. The assembly was then immersed into a liquid nitrogen bath, as shown in Fig. 7, for testing. For the TMO-I and natural samples, only single-side tests were performed, however, for the ice a double-sided test was performed.



Fig. 7. Styrofoam and a C-clamp securing the sample to the Hot Disk sensor with entire assembly submerged into a liquid nitrogen bath.

RESULTS AND DISCUSSIONS

THERMAL CONDUCTIVITY OF ICE

In the first test, the standard Hot Disk method was used where the Kapton sensor/heater was sandwiched between the two ice specimens. The test conditions were: 0.5 Watt and 10 seconds and at -34°C the average thermal conductivity was 2.39 W/mK . For measuring the thermal conductivity near -194°C the sample holder was placed into a liquid nitrogen bath. The average thermal conductivity for ice in a liquid nitrogen bath is 8.45 W/mK . The results are plotted with published thermal conductivity values [6] in Fig. 8. The increase in thermal conductivity at lower temperatures is typical behavior for crystalline materials. The test of ice proved that the Hot Disk method could be used at liquid nitrogen temperatures.

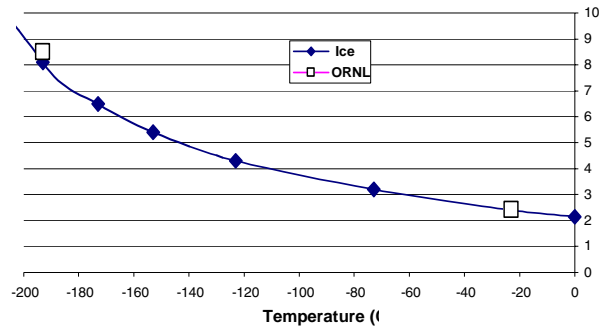


Fig. 8. Thermal conductivity of ice at low temperatures.

TMO-I AND NATURAL SAMPLES

A TMO-I sample was used in the single-side test backed by Styrofoam. The thermal conductivity tests conducted at -34°C showed a value of 0.58 W/mK . At liquid nitrogen temperature, -194°C , the average thermal conductivity was 0.49 W/mK . The decrease in thermal conductivity as a function of temperature is consistent with THF hydrate in the literature [7]. The literature values of THF is shown in Fig. 9 as a reference since no such TMO-I thermal conductivity values were available to us.

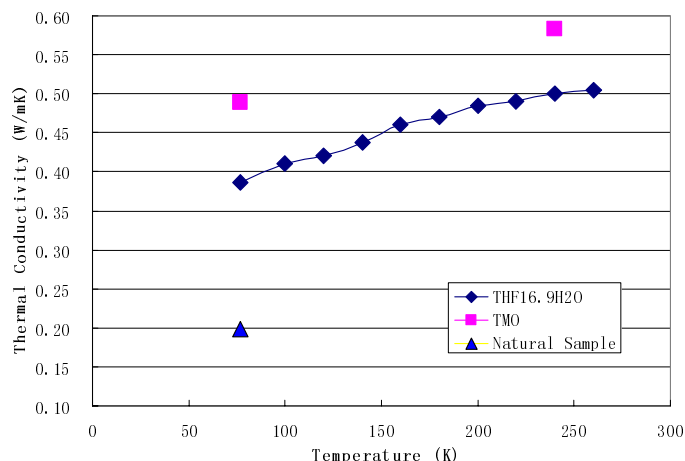


Fig. 9. Thermal conductivity of TMO-I and natural samples.

The only two larger natural samples (collected from two different sites) did not match well in size for the standard test.

The natural samples showed an even lower thermal conductivity at liquid nitrogen temperature. The average value was 0.20 W/mK with relatively large scatter (15–20%). This was due to the fact that thermal conductivity of natural sample is comparable to the backing Styrofoam and the reduced thermal conductivity contrast resulted more uncertainty in the measurements. The ideal condition will be testing two natural samples using the

INFRARED TEMPERATURE MONITORING OF NATURAL CLATHRATE HYDRATE SAMPLES UNDER HIGH PRESSURE

Hsin Wang

Proper handling natural of samples is the key to characterization efforts. Since the melting temperature of the natural samples are well below ambient temperature, the control of temperature during measurements, transport and handling becomes very important. Currently, the natural samples are stored at liquid nitrogen temperature and a small amount of sample is taken out for data collection. There has been no effective temperature monitoring during the measurements other than cell or environment temperatures. We employed an infrared camera to monitor sample temperatures in a high-pressure sapphire cell. The following are some preliminary IR images and analysis.

EXPERIMENTS

The high-pressure cell has been described in other reports related to this study [1]. The cell is made of sapphire, which is an infrared transparent material. We used a Raytheon, Radiance HS, IR camera in this study. The IR camera has a 256 × 256 pixel Focal Plane Array InSb detector, which is sensitive to 3–5 micron thermal radiation. At room temperature, the 12-bit digital image gives a temperature resolution of 0.015°C. For this preliminary study temperature calibration was not performed since it

requires more experimental effort and we are only interested in relative temperature changes at this stage. The integration time of the IR camera was 1 ms.

Typical IR monitoring consists 3–4 minutes continuous temperature measurements at 1 Hz. The digital image sequences were played back and analyzed by Image Desk software.

During the experiment, a small piece of natural sample was taken from a liquid nitrogen bath and quickly inserted into the cell. Once the cell top was secured, high pressure was applied to keep the sample from melting. The IR camera started collecting images from a distance. This type of non-contact temperature measurement can be used while conducting other measurements.

RESULTS AND DISCUSSION

Figure 10 shows the temperature images of a natural sample under pressure (a) in the beginning, (b) 4 minutes later. The plots on the right are line-temperature-profiles indicated by the black lined going through the sample. The temperature was not calibrated for emissivity. The background, room temperature, intensity was about 1700. For a material with emissivity close to 1, $1^{\circ}\text{C} = 30$ intensity units. Using this estimate, the sample temperature in Fig. 10(a) was at least 12°C below room temperature. Note in Fig. 10(b) the sample was partially melted and the temperature scale increased 100 units (at least 3°C).

In Fig. 11, a small circular area, “1” was monitored over time, the maximum, minimum, and average temperatures in that area were plotted on the right. All three temperatures showed a jump after 40 seconds. This was because a step-increase in cell pressure. Even at constant pressure, the IR camera still observed melting of the sample, especially in the areas in contact with the cell wall and the support.

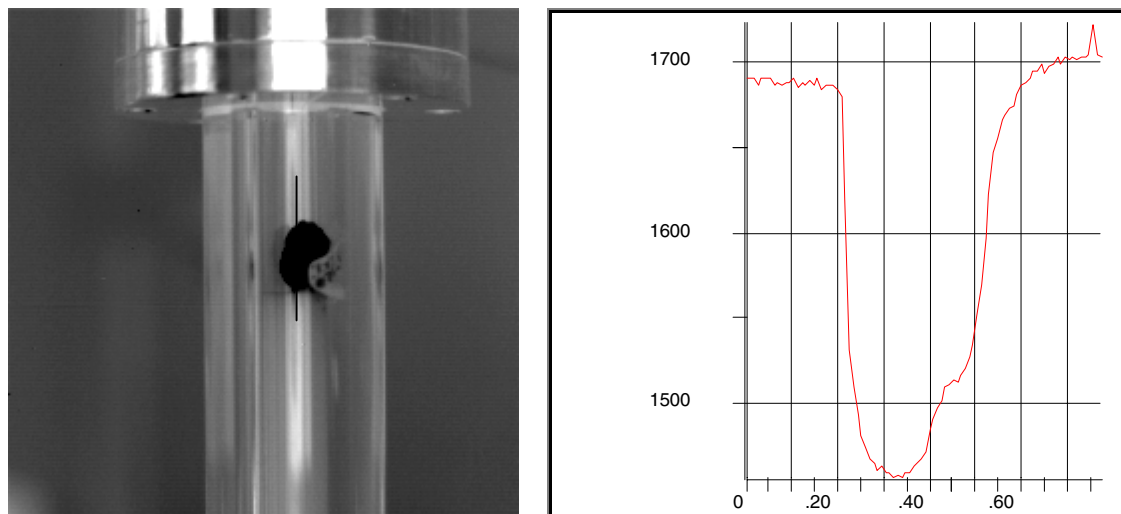


Fig. 10 (a) Natural sample in a high pressure sapphire cell. Temperature is shown in uncalibrated IR intensity scale.

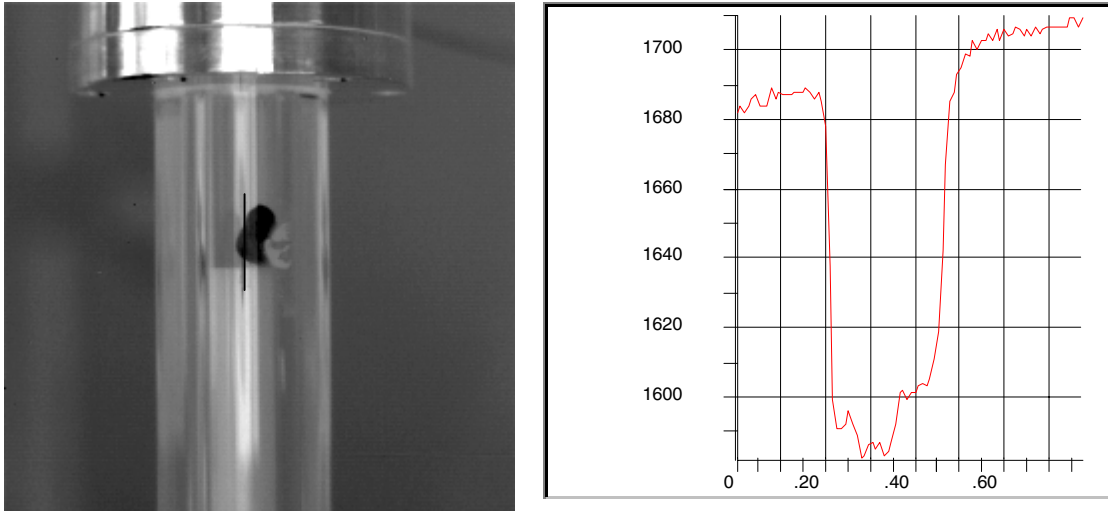


Fig. 10 (b) Same natural sample 4 minutes later. About half of the sample has melted away. The temperature of the sample increased 100 unit (3–4 degree C).

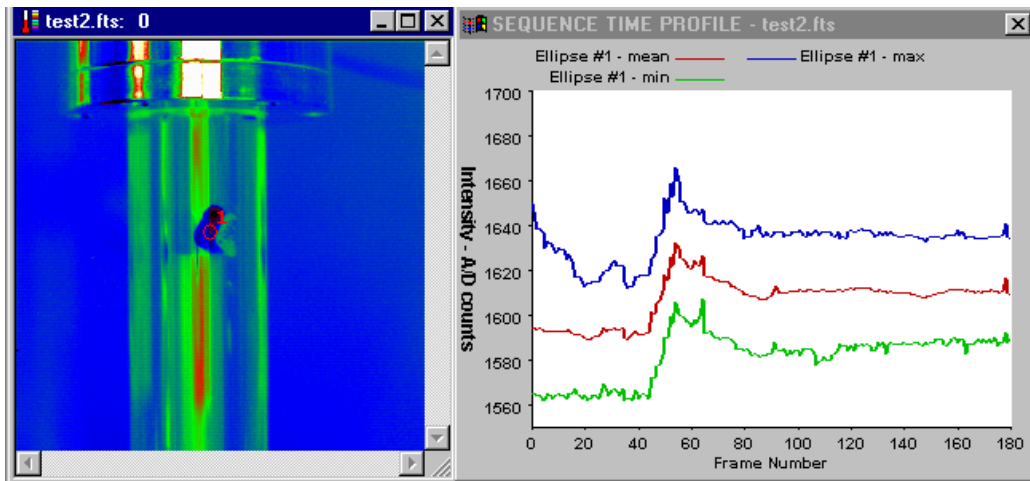


Fig. 11. Temperature changes (max, min and average) of a natural sample under pressure over a period of 3 minutes (imaging speed at 1 Hz) in a circular area “1”. The temperature jump after 40 seconds was due to a step increase in cell pressure.

Figure 12 shows the temperature change of a natural sample when the cell pressure was released. A single point temperature, “2”, was traced and plotted on the right. The sample temperature kept dropping for at least 25 seconds after the pressure release.

Other than, pressure change in the cell, the sample temperature was also affected by direct contact with the cell wall and supporting rod. The heat transfer from contact is one source of continuous melting of the sample even when the sample is under constant pressure. Detailed study requires careful calibration and control of the experiments.

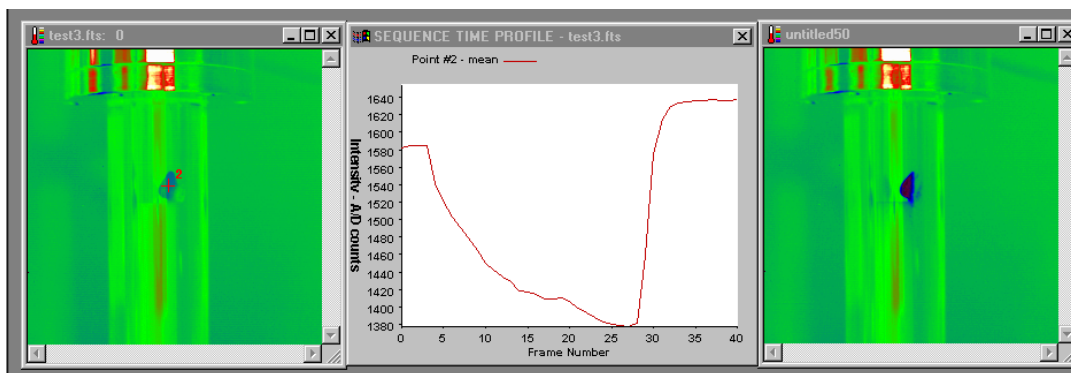


Fig. 12. IR imaging of natural sample melting after pressure release. The sample temperature kept dropping for 25 seconds.

SUMMARY

This was a preliminary study to explore the feasibility of using IR imaging in our study of natural sample. The results showed this method can be used as an effective tool to monitor sample temperature changes during data collection. The time-stamped temperature maps will help us in explaining experimental results of the natural samples.

AMERICAN MINERALOGIST CLATHRATE HYDRATE SPECIAL ISSUE

Bryan C. Chakoumakos

Through discussions with the Editor, Lee Groat, from the University of British Columbia, the American Mineralogist has embraced the idea to publish a special issue devoted to clathrate hydrates. The publication date is set to be October 2004, with a manuscript submission deadline of October 2003. Roughly thirty hydrate researchers have agreed to contribute, from a solicitation of over 400 researchers worldwide. The American Mineralogist, the premier International Journal of Earth and Planetary Sciences and the official publication of the Mineralogical Society of America, publishes the results of original research in the general fields of mineralogy, crystallography, petrology, and geochemistry. Journal details and information for authors are available at <http://www.minsocam.org/MSA/AmMin/AmMineral.html>. Each manuscript submission will be subject to the same peer review process as regular articles. The special issue will have space to accommodate 20 to 30 articles. Bryan Chakoumakos (Oak Ridge National Laboratory) will act as a managing editor.

Topics that will be included for this special issue are crystal structure, physical property measurements, kinetic studies, thermodynamical properties, phase equilibria, natural occurrence descriptions, synthetic analogs, high pressure studies, experimental methods, theoretical modeling, carbon dioxide sequestration, etc.

INELASTIC NEUTRON SCATTERING OF CLATHRATE HYDRATES

Bryan Chakoumakos

Vibrational spectroscopy of clathrate hydrates links the microscopic properties to the macroscopic properties, such as thermal conductivity. Vibrational spectroscopy done by inelastic neutron scattering (INS) generally offers poorer resolution than FTIR or Raman, but it has no selection rule restrictions. Examples INS spectra of a clathrate hydrate (TMO structure I) collected on a triple-axis spectrometer at several temperatures are shown in Fig. 13. The incoherent scattering is so much larger for the hydrogen as compared to the other constituent atoms of typical clathrate hydrates that it overwhelmingly dominates the contribution to the spectra. Consequently, for a synthetic sample prepared with a deuterated host lattice, the INS spectrum will emphasize those vibrational modes involving the hydrogenous guest molecule. In contrasting synthetic samples prepared with and without a deuterated host lattice, Fig. 14, some modes shift in frequency whereas others do not, which in principle should help to identify which modes are associated with the guest molecule, host lattice, or both. Our preliminary experiments of synthetic samples show that in the low energy transfer region (0–50 meV) there are prominent modes connected to the guest host coupling. We have examined two natural structure II methane hydrates from Green Canyon in the Gulf of Mexico over the 0–50 meV energy transfer range. As these samples are hydrogenous, and contain small amounts of higher

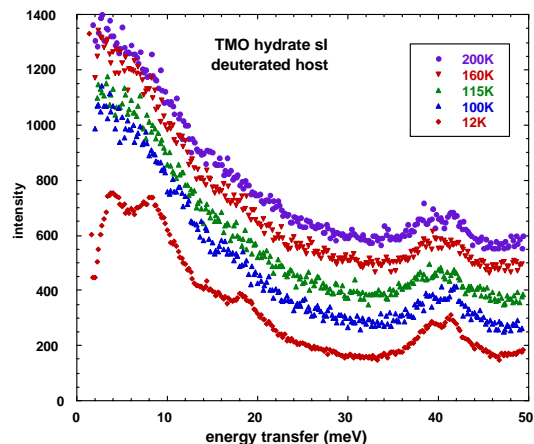


Fig. 13. Inelastic neutron scattering spectra for trimethylene oxide (TMO) hydrate sI as a function of temperature. The host lattice is deuterated and the guest molecule is hydrogenous. The spectra are offset along the vertical axis for clarity. Data collected on the HB1 triple-axis spectrometer at the HFIR, ORNL.

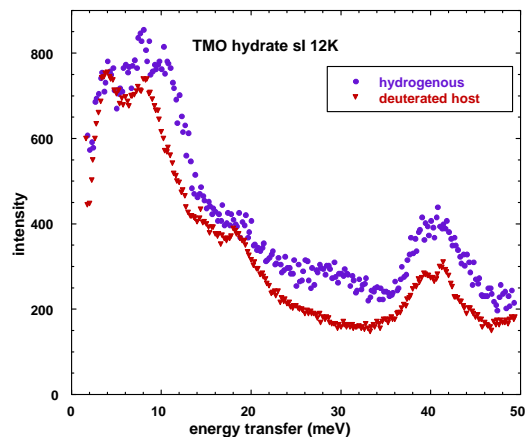


Fig. 14. Inelastic neutron scattering spectra for trimethylene oxide (TMO) hydrate sI at 12K comparing a fully hydrogenous sample with one that has only a deuterated host lattice. The spectra are offset along the vertical axis for clarity. Data collected on the HB1 triple-axis spectrometer at the HFIR, ORNL.

weight hydrocarbon molecules, the INS do not show as much detail as the purely synthetic samples [Fig 15(a) and (b)]. Nevertheless, the spectra do exhibit changes as a function of temperature and some structure at the lowest energy transfers. To fully identify the various vibrational modes in the spectra, it will be necessary to undertake higher resolution scans with different neutron spectrometers, correlate the spectra with Raman and IR measurements, and examine more synthetic samples (both deuterated and hydrogenous). This month, Yoshi Ishii is undertaking new INS of a fully hydrogenous sI methane hydrate freshly synthesized by the U.S. Geological Survey (Stern et al.) on a higher resolution spectrometer at the Japan Atomic Energy Research Institute. His results will be integrated into the interpretation of our own preliminary measurements, and devising the most appropriate instrument design for future measurements. Ultimately, we can expect to further elucidate the underlying lattice dynamical picture of the glass-like thermal conductivity exhibited by the gas clathrate hydrates.

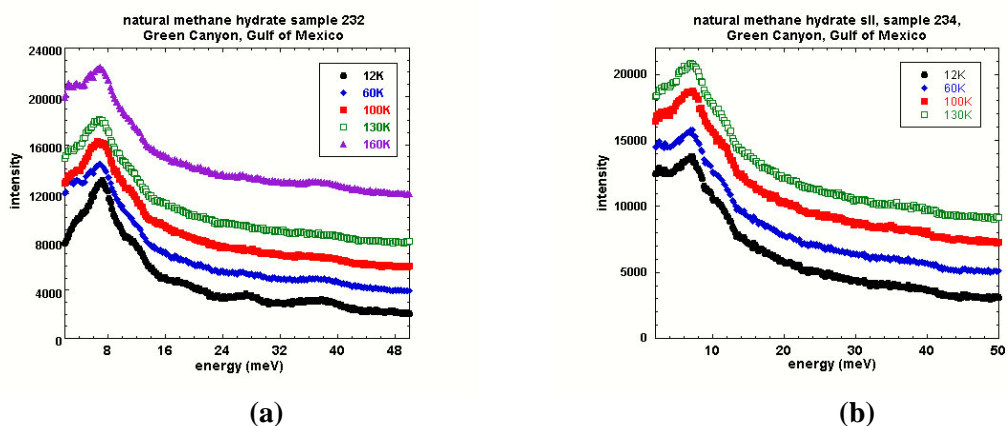


Fig. 15. Inelastic neutron scattering spectra for methane hydrate sII samples (a) 232 and (b) 234 from Green Canyon, Gulf of Mexico. The spectra are offset along the vertical axis for clarity. Data collected on the HB1 triple-axis spectrometer at the HFIR, ORNL.

RAMAN SCATTERING MEASUREMENTS

Michael Lance and Adam J. Rondinone

Raman microscopy is extremely useful in characterizing gas hydrates since it can directly measure the vibrational energies of the interstitial gas molecules non-destructively. Also, since the Raman spectroscopy is a scattering spectroscopy, spectra can be obtained through a clear pressure cell for in-situ measurements at various temperatures and pressures. In addition, the spot size is $\sim 2 \mu\text{m}$, which allows one to probe around microstructural features of natural samples.

Raman spectra were obtained with a DilorXY800 triple stage Raman microprobe (JY, Inc., Edison, NJ) using a Innova 308C Ar⁺ ion laser (Coherent Laser Group, Santa Clara, CA) at 5145 Å and 100mW output power. The spot diameter and penetration depth were both ~2 μm in size. Both a high pressure cell (Sam O. Colgate, Inc., Gainesville, FL) and a low temperature stage (THMS 600, Linkam, Inc.), were used to create and analyze gas hydrates.

The high-pressure cell has a maximum pressure of 10,000 psi at 25°C and can be cooled to -20°C. A thermocouple inside the cell measures the temperature and a magnetic stirrer ensures a well-mixed solution. The initial test showed that we successfully created the methane hydrate at 5100 psi and 4°C. The peak from the methane hydrate structure I and a shoulder from structure II (see Fig. 16) were clearly visible showing that we successfully created gas hydrate. The peak positions compared well with values reported in the literature.

Natural hydrate samples (GC232 and GC234) were analyzed at low temperatures using the cooling stage. Sample GC232 had more petroleum deposits and visually looked dirtier than sample GC234. This resulted in a slightly higher background for this sample but Raman spectra could still be acquired. The effect of temperature on the Raman peak position of the structure I methane hydrate is shown in Fig. 17. The peak shifts only ~0.5 cm⁻¹ over a 60°C temperature range which shows that the temperature where we choose to measure will have little effect on our measured peak positions and so can be compared to literature values.

The spectra obtained from sample GC234 is shown in Fig. 18(a) and (b) for the spectral ranges associated with C-H vibrations and with C-C vibrations, respectively. Numerous peaks are observed which are related to various gases and are summarized in Table 1. Methane and ethane were the predominant gases along with trace amounts of isobutene and trans-butane. The methane and ethane were observed in both structures I and II. Raman bands from sample GC232 are essentially identical to those from sample GC234.

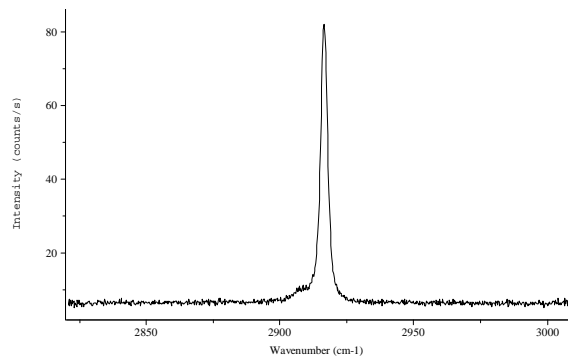


Fig. 16. Raman spectrum obtained from methane hydrate at 2100 psi and 16°C.

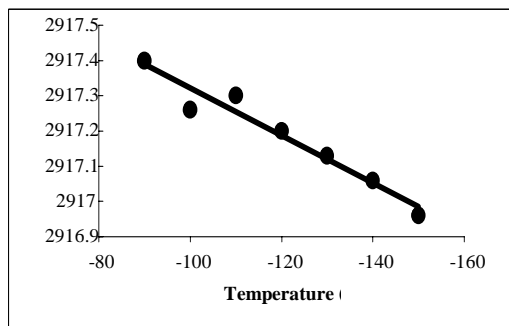


Fig. 17. Effect of temperature on the peak position of the structure I methane hydrate.

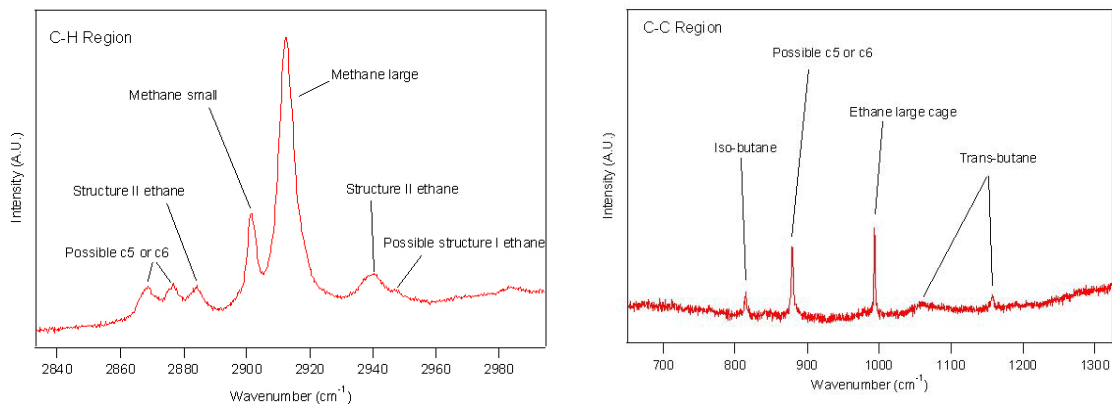


Fig. 18. Raman spectrum from natural sample GC234 in the spectral region associated with (a) C-H vibrations and (b) C-C vibrations.

Table 1. Assignment of Raman bands to different gas hydrates in natural samples

<i>Possible Clathrate 1st Guess</i>	<i>Measured Peak Position (cm⁻¹)</i>	<i>From Literature</i>
C5 or C6	2868.49	
C5 or C6	2876.71	
C2H6 in SII 5(12)6(2) Large	2884.34	2887.3
CH4 in SII 5(12)6(4) Large	2898.77	2903.72 +/- 0.28
CH4 in SI 5(12)6(2) Large	2901.73	2904.85 +/- 0.33
CH4 in SII 5(12) Small	2912.32	2913.73 +/- 0.76
CH4 in SI 5(12) Small	2917.14	2915.04 +/- 0.58
C2H6 in SII 5(12)6(2) Large	2939.47	2942.3
C2H6 in SI 5(12)6(2) Large	2947.46	2946.2
???	2982.53	

SMALL-ANGLE NEUTRON SCATTERING OF NATURAL CLATHRATE HYDRATES

Jane Y. Howe and Camille Y. Jones

EXPERIMENTAL PROCEDURES

Small Angle Neutron Scattering (SANS) experiments were carried out at National Center for Neutron Research at National Institute of Standard and Technology, Gaithersburg, MD. Data were collected on the NG3, a 30-m SANS instrument equipped with a helium closed-cycle refrigerator (CCR), with a monochromatic neutron influx at wavelength of 6.0 Å, and a momentum transfer Q from 0.004 to 0.47 Å⁻¹. The sample holder is made of aluminum with a path length of 1 mm. Data was collected on sample GC234 at 25, 50, 75, 100, and 125 K and on samle GC232 hydrates at 25, 75, and 125 K. Scattering from the empty cell was measured at 25 and 125 K. Data was also collected on sediment samples from the vicinities of both the GC232 and GC234 mounds. These samples were dried in air around 340 K and ground to fine powder prior to the SANS study. The sediment part of the GC232

sample, which remained after the decomposition of the hydrates and gases, was also studied. The SANS data of mud and sediment samples were collected at 283 and 298 K with 1 mm path length. SANS data analysis was carried out using the SANS Analysis Package with IGOR, developed by S.R. Kline which is available at NIST's website [8].

RESULTS AND DISCUSSION

SANS data of GC232 and GC234 hydrates, plotted in log-log format, are compiled in Figs. 19 and 20. These data were collected from 0.002 to 0.32 \AA^{-1} that covers the structural characteristics in the mesoscale range (~ 2 to 300 nm). Both samples show the temperature independence of small-angle scattering. And both samples have the power-law relationship; the slope of the power-law fit is 3.4 for GC234 and 3.3 for GC232 (Table 2). This indicates that the samples are surface fractal with a surface fractal dimension of 2.6 and 2.7 respectively.

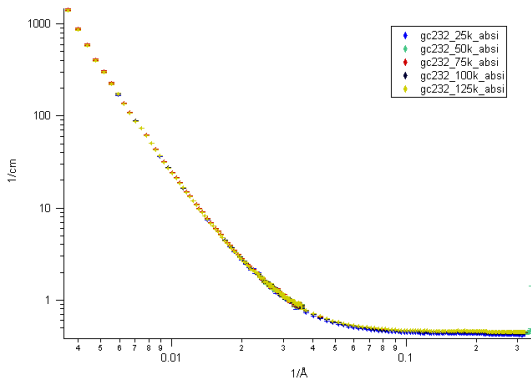


Fig. 19. SANS data of GC232 taken at 25 to 125K.

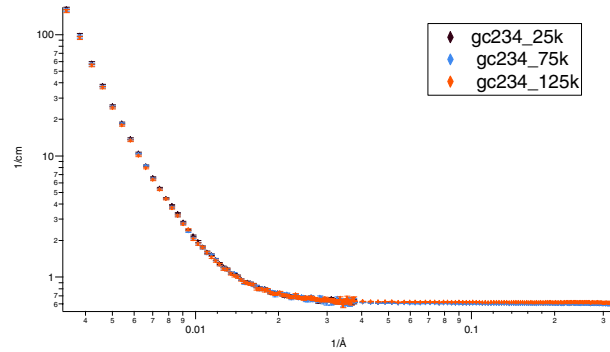


Fig. 20. SANS data of GC234 taken at 25, 75 and 125K, which indicates the temperature independence.

Table 2. SANS data Analysis

	Two-phase model Cor. Length (nm) χ^2		Power-Law α	Fractal D_s ($6-\alpha$)
GC234-25K	68	5.6	3.4	2.6
GC234-75K	72	4.5	3.4	2.6
GC234-125K	72	3.4	3.4	2.6
GC232-25K	23	96.3	3.3	2.7
GC232-75K	22	120.6	3.3	2.7
GC232-125K	22	119.8	3.3	2.7

GC234 is the sample with little sediment. XRD reveals that it is a mix of type II hydrate and ice in 70:30 wt ratio. Hence, it is reasonable to describe the small-angle data using the Debye-Bueche model.

The correlation length is calculated to be 68, 72, and 72 nm for GC234 at 25, 75, and 125 K, respectively (Table 2). The value of χ^2 quantifies the goodness of a fit. The small value of χ^2 for the GC234 data suggests that the model and experimental results agrees quite well.

Figure 21 contains plots of GC232 and GC234 data taken at 25 K. The scattering intensity of the GC232 extends to a higher Q-range, suggesting that the structural feature is smaller that of GC234. The GC232 data were fitted to the two-phase Debye-Bueche model and the correlation length was estimated to be 22 nm. The fitness of the data is poor as the value of χ^2 is 120, implying that GC232 is not a two-phase system and that a more complicated model needs to be used.

The SANS data of the sediment and the GC232 are compared in Fig. 22. Data analysis indicates that the sediment sample has smaller correlation length at 14 nm. A better interpretation of the SANS data is possible once the structural information and chemical composition (XRD and ND results) becomes available.

SUMMARY

GC234 is a two-phase system of hydrate and ice mix and well described using the Debye-Bueche model. The correlation length is calculated to be 70 nm. The correlation length of the GC232 is 22 nm, though the fitting of the Debye-Bueche model is relatively poor.

REFERENCES

1. A. J. Rondinone, C. Y. Jones, S. L. Marshall, B. C. Chakoumakos, C. J. Rawn, and E. Lara-Curizo, "A Single-Crystal Sapphire Cell for in situ Neutron Diffraction Study of Gas-Hydrate," in press *Can. J. Phys.* (2002).
2. C. J. Rawn, A. J. Rondinone, B. C. Chakoumakos, S. Circone, L. A. Stern, S. H. Kirby, and Y. Ishii, "Neutron Powder Diffraction Studies as a Function of Temperature of Structure II Hydrate Formed from Propane," in press *Can. J. Phys.* (2002).

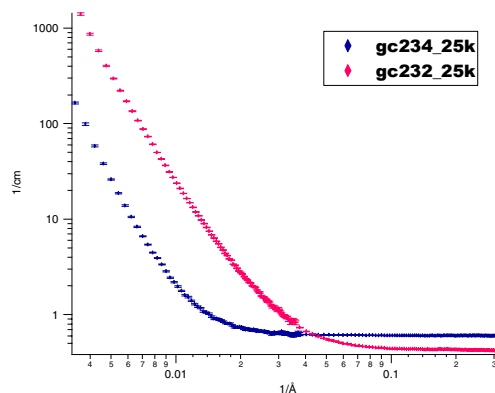


Fig. 21. The SANS data of GC232 and GC234 taken at 25 K.

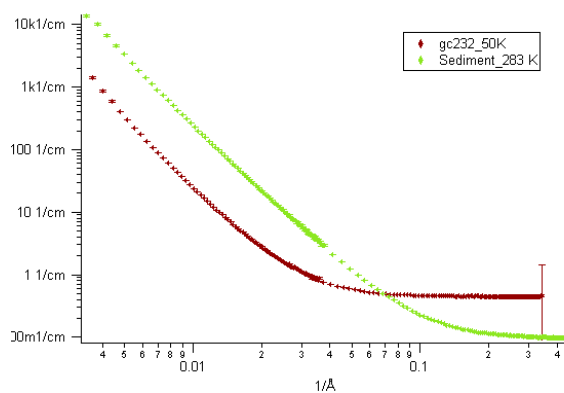


Fig. 22. The SANS data of GC232 hydrate and its sediment.

3. B. C. Chakoumakos, C. J. Rawn, A. J. Rondinone, L. A. Stern, S. Sircone, S. H. Kirby, Y. Ishii, C. Y. Jones, B. H. Toby, and D. C. Dender, "Temperature Dependence of Polyhedral Cage Volumes in Clathrate Hydrates," in press *Can. J. Phys.* (2002).
4. C. Y. Jones, S. L. Marshall, B. C. Chakoumakos, C. J. Rawn, and Y. Ishii, "Structure and Thermal Expansivity of Tetrahydrofuran Deuterate Determined by Neutron Powder Diffraction," accepted *J. Phys. Chem. B* (2002).
5. C. J. Rawn, A. J. Rondinone, B. C. Chakoumakos, S. L. Marshall, L. A. Stern, S. Sircone, S. H. Kirby, C. Y. Jones, B. H. Toby, and Y. Ishii, "Neutron Powder Diffraction Studies as a Function of Temperature of Structure II Hydrate Formed from a Methane + Ethane Gas Mixture," *Proceedings of the Fourth International Conference on Gas Hydrates* (2002), p. 595.
6. G. A. Slack, "Thermal Conductivity of Ice," *Physic. Rev. B.* **22**(6), 3065–3071, 1980.
7. H. Suga, "Calorimetric Studies of Some Energy-Related Materials," *Thermochimica Acta*, **328**, 9–17, 1999.
8. S.R. Kline, SANS Analysis with IGOR
http://www.ncnr.nist.gov/programs/sans/manuals/data_anal.html